Structural Analysis of Orthotropic Shells

GEORGE G. LOVE*
General Motors Corporation, Indianapolis, Ind.

A method of analysis is presented for stresses in axisymmetrically loaded orthotropic surfaces of revolution. The equations are given in a form readily adaptable to a computer solution by a process of numerical integration. Particular emphasis is given to filament-wound pressure vessels where a method of minimizing the discontinuity stresses at the cylinder to dome juncture is described. Numerical results of the analysis are compared with values obtained from the hydrotest of a filament-wound structure.

Nomenclature

A_{ij} = elastic constants of material [defined by Eq. (5)]
a = radius of cylinder; radius of dome at tangent point
E = Young's modulus
G = shear modulus
h = thickness
K = curvature
M = moment
N = membrane force
p = internal pressure
Q = shear
r = radius of curvature
S = slope
v = deflection in meridional direction
w = deflection normal to surface
x, y = coordinates of dome contour
Z = dome form factor
z = coordinate in direction of thickness
α = helix angle
γ = shear strain
ϵ = strain
σ = stress
λ = defined in Eq. (1)
ν_{BA} = Poisson's ratio (ratio of contraction in A direction to elongation in B direction when loaded in B direction)
τ = shear stress
ϕ = reference angle (defined in Fig. 3)

Subscripts

A, B = natural axes of orthotropic material
m = meridional direction
0 = at tangent point
t = tangential (circumferential) direction

Introduction

IN recent years, the use of reinforced plastics as structural materials has become widespread. In particular, pressure vessels have been fabricated by the filament-winding process in which continuous glass fibers are wound over a suitable mandrel and are bonded together by an epoxy resin. The high strength-to-weight ratio of this type of structure makes it particularly suitable for such applications as rocket-motor cases.

Since 1957, the Allison Division of General Motors Corporation has been engaged in the design and fabrication of steel and titanium rocket-motor cases. In 1960, the scope of this work was extended to include filament-wound cases. A company-sponsored program was initiated, under which a winding machine was developed and a 44-in.-diam case and numerous subscale bottles were fabricated and tested. The analytical work associated with this program forms the basis of this paper.

In general, filament-wound structures display a symmetry with respect to the principal axes. Thus, the resulting material is orthotropic. The basic elastic relationships for orthotropic materials are well known.[1] Similarly, dome contours for filament-wound pressure vessels have been described in the literature.[2,3] Both of these subjects are discussed in this report for the sake of continuity.

Elastic Relationships

Consider first an element of a material composed of unidirectional filaments embedded in a matrix. Let the direction of the filaments be parallel to the A axis (Fig. 1).

It is assumed that the composite may be treated as a homogeneous orthotropic material so that, under biaxial loading, the following stress-strain relationships apply:

$$\begin{aligned} \sigma_A &= (E_A/\lambda)[\epsilon_A + \nu_{BA}\,\epsilon_B] \\ \sigma_B &= (E_B/\lambda)[\nu_{AB}\,\epsilon_A + \epsilon_B] \\ \tau_{AB} &= G_{AB}\,\gamma_{AB} \end{aligned} \qquad (1)$$

where $\lambda = 1 - \nu_{AB}\,\nu_{BA}$. The stresses referred to the natural axes A and B can be transformed into stresses referred to an arbitrary axis system, m and t, which is displaced through an angle α from the A-B system (Fig. 2).

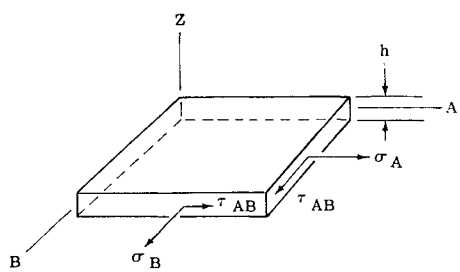

Fig. 1 Element of orthotropic material.

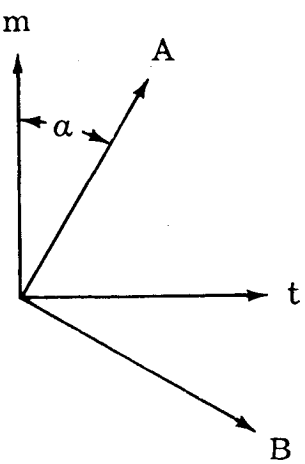

Fig. 2 Reference axes.

Presented at the AIAA Launch and Space Vehicle Shell Structures Conference, Palm Springs, Calif., April 1–3, 1963. The author wishes to thank H. E. Helms and R. L. Stedfeld for their helpful suggestions and comments on the preparation of this paper.

* Senior Project Engineer, Allison Division.

The transformation from one axis system to the other is given by the following relationships:[1]

$$\begin{aligned}\sigma_m &= \sigma_A \cos^2\alpha + \sigma_B \sin^2\alpha - 2\tau_{AB} \sin\alpha \cos\alpha \\ \sigma_t &= \sigma_A \sin^2\alpha + \sigma_B \cos^2\alpha + 2\tau_{AB} \sin\alpha \cos\alpha \\ \tau_{mt} &= \sigma_A \sin\alpha \cos\alpha - \sigma_B \sin\alpha \cos\alpha + \tau_{AB}(\cos^2\alpha - \sin^2\alpha)\end{aligned} \tag{2}$$

Similarly, the strains are related by

$$\begin{aligned}\epsilon_A &= \epsilon_m \cos^2\alpha + \epsilon_t \sin^2\alpha + \gamma_{mt} \sin\alpha \cos\alpha \\ \epsilon_B &= \epsilon_m \sin^2\alpha + \epsilon_t \cos^2\alpha - \gamma_{mt} \sin\alpha \cos\alpha \\ \gamma_{AB} &= -2\epsilon_m \sin\alpha \cos\alpha + 2\epsilon_t \sin\alpha \cos\alpha + \gamma_{mt}(\cos^2\alpha - \sin^2\alpha)\end{aligned} \tag{3}$$

The stress-strain relationships in the m, t coordinate system may be written in the form:

$$\begin{aligned}\sigma_m &= A_{11}\,\epsilon_m + A_{12}\,\epsilon_t + A_{13}\,\gamma_{mt} \\ \sigma_t &= A_{21}\,\epsilon_m + A_{22}\,\epsilon_t + A_{23}\,\gamma_{mt} \\ \tau_{mt} &= A_{31}\,\epsilon_m + A_{32}\,\epsilon_t + A_{33}\,\gamma_{mt}\end{aligned} \tag{4}$$

The coefficients A_{ij} may be found by substituting Eqs. (1) and (3) into Eq. (2). This results in coefficient values as follows:

$$\begin{aligned}A_{11} &= (1/\lambda)[E_A \cos^4\alpha + E_B \sin^4\alpha + 2 \sin^2\alpha \cos^2\alpha(E_B \nu_{AB} + 2 G_{AB}\lambda)] \\ A_{12} = A_{21} &= (1/\lambda)[E_B \nu_{AB}(\cos^4\alpha + \sin^4\alpha) + \sin^2\alpha \cos^2\alpha(E_A + E_B - 4 G_{AB}\lambda)] \\ A_{13} = A_{31} &= (1/\lambda)[\sin\alpha \cos^3\alpha(E_A - E_B \nu_{AB} - 2 G_{AB}\lambda) - \sin^3\alpha \cos\alpha(E_B - E_B \nu_{AB} - 2 G_{AB}\lambda)] \\ A_{22} &= (1/\lambda)[E_A \sin^4\alpha + E_B \cos^4\alpha + 2 \sin^2\alpha \cos^2\alpha(E_B \nu_{AB} + 2 G_{AB}\lambda)] \\ A_{23} = A_{32} &= (1/\lambda)[\sin^3\alpha \cos\alpha(E_A - E_B \nu_{AB} - 2 G_{AB}\lambda) - \sin\alpha \cos^3\alpha(E_B - E_B \nu_{AB} - 2 G_{AB}\lambda)] \\ A_{33} &= (1/\lambda)[\sin^2\alpha \cos^2\alpha(E_A + E_B - 2E_B \nu_{AB}) + (\cos^2\alpha - \sin^2\alpha)^2 G_{AB}\lambda]\end{aligned} \tag{5}$$

In obtaining Eqs. (5), use has been made of the reciprocal relationship:

$$(E_A/E_B) = (\nu_{AB}/\nu_{BA}) \tag{6}$$

Consider now a laminate composed of several layers. By assuming that the layers are connected by a material that has infinite shear rigidity (i.e., the strains are uniform over the total thickness), the effective elastic constants of the laminate are given by

$$\bar{A}_{ij} = \frac{1}{h} \sum_{k=1}^{n} A_{ijk} h_k \tag{7}$$

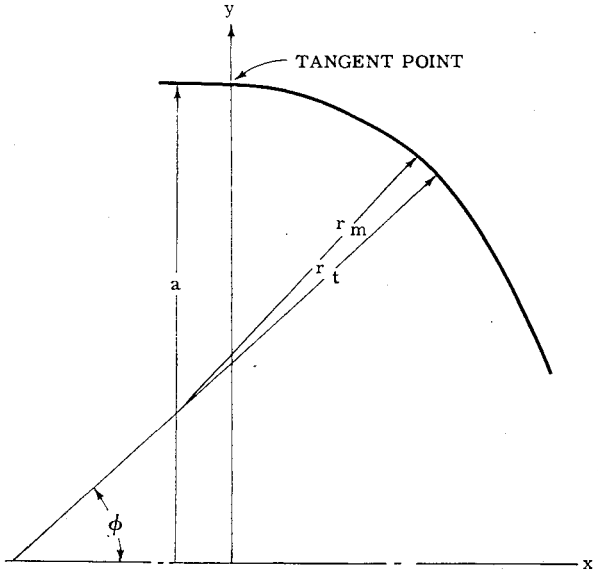

Fig. 3 Dome geometry.

where n = number of layers, h = total thickness, $i = 1, 2, 3$, and $j = 1, 2, 3$.

Filament-Wound Structures

The following discussion is restricted to a laminate in which the layers display symmetry with respect to the m and t axes of the laminate. That is, the number of layers oriented at an angle α is equal to the number of layers oriented at an angle $-\alpha$. In general, filament-wound structures fall into this classification.

Let the m and t axes correspond to the meridional and tangential (circumferential) axes of a filament-wound pressure vessel. From symmetry, $\gamma_{mt} = 0$. The stress-strain relationships now may be written in the form:

$$\begin{aligned}\sigma_m &= (\bar{E}_m/\bar{\lambda})[\epsilon_m + \bar{\nu}_{tm}\,\epsilon_t] \\ \sigma_t &= (\bar{E}_t/\bar{\lambda})[\bar{\nu}_{mt}\,\epsilon_m + \epsilon_t]\end{aligned} \tag{8}$$

where $\bar{\lambda} = 1 - \bar{\nu}_{mt}\,\bar{\nu}_{tm}$. Then, from Eqs. (4) and (8),

$$\begin{aligned}\bar{E}_m &= \bar{A}_{11} - (\bar{A}_{12}^2/\bar{A}_{22}) \qquad \bar{\nu}_{mt} = \bar{A}_{12}/\bar{A}_{22} \\ \bar{E}_t &= \bar{A}_{22} - (\bar{A}_{12}^2/\bar{A}_{11}) \qquad \bar{\nu}_{tm} = \bar{A}_{12}/\bar{A}_{11}\end{aligned} \tag{9}$$

These expressions are used in subsequent sections.

Dome Contour

The coordinate axes and notation used in the following discussions are shown in Fig. 3. The ideal dome contour of a filament-wound pressure vessel is one in which the filaments are loaded in pure tension. Use of the membrane load relationship,

$$N_t/N_m = 2 - (r_t/r_m) \tag{10}$$

leads to the well-known dome contour equation[3]:

$$y''y = [1 + (y')^2][(N_t/N_m) - 2] \tag{11}$$

where the primes denote differentiation with respect to x.

The "netting" analysis, commonly used in establishing dome contours, uses the condition that, for balanced loading,

$$N_t/N_m = \tan^2\alpha \tag{12}$$

where α is the "local" helix angle. However, when the effect of the resin is taken into account, a balanced stress condition may be defined by setting σ_B equal to zero. Then, from Eq. (1),

$$\epsilon_B = -\nu_{AB}\,\epsilon_A \tag{13}$$

Combining Eqs. (3) and (13) and letting $\gamma_{mt} = 0$ gives

$$\frac{\epsilon_m}{\epsilon_t} = -\frac{(\nu_{AB} \tan^2\alpha + 1)}{\nu_{AB} + \tan^2\alpha} \tag{14}$$

Letting $\sigma_m = N_m/h$ and $\sigma_t = N_t/h$, from Eq. (4),

$$\frac{N_t}{N_m} = \frac{A_{12}(\epsilon_m/\epsilon_t) + A_{22}}{A_{11}(\epsilon_m/\epsilon_t) + A_{12}} \tag{15}$$

By combining Eqs. (14) and (15) and using the notation of Eq. (9) one obtains

$$\frac{N_t}{N_m} = \frac{\bar{E}_t}{A_{11}}\left[\frac{\nu_{AB} + \tan^2\alpha}{\tan^2\alpha(\bar{\nu}_{tm} - \nu_{AB}) + \bar{\nu}_{tm}\,\nu_{AB} - 1}\right] + \bar{\nu}_{tm} \tag{16}$$

Thus, substitution of Eq. (16) into Eq. (11) gives the equation of a dome contour for which σ_B is zero at every point.

Discontinuity Stresses

By considering the dome to act as a membrane, the free edge deflection of the tangent point ($x = 0$) due to internal pressure may be expressed as

$$w_0 = (p\,a^2/2\bar{E}_t h)[\bar{\nu}_{tm} - (N_t/N_m)] \tag{17}$$

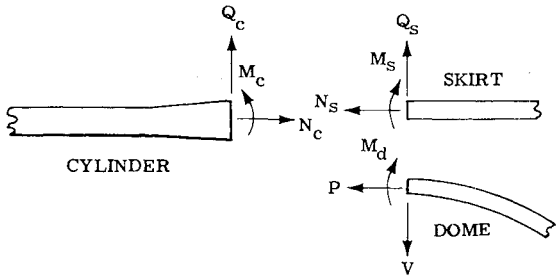

Fig. 4 Free body of juncture.

The wrapping angle and the properties of the materials commonly used for filament-wound pressure vessels are such that the deflection as given by Eq. (17) is radially inward. Since the cylindrical portion of the vessel tends to deflect radially outward, bending will occur at the juncture of the dome and cylinder, producing an unbalanced stress condition.

The deflection discontinuity can be reduced by increasing the meridional radius of curvature, r_m, in the region of the tangent point, thereby increasing the ratio N_t/N_m [see Eq. (10)]. But, for a balanced stress condition ($\sigma_B = 0$), N_t/N_m is specified by Eq. (16). Thus, while the σ_B due to the discontinuity is decreased, that due to the membrane loads is increased. However, the net reduction in σ_B can be quite significant.

The ratio N_t/N_m may be increased by arbitrarily adding a quantity $(2 - Z)$ to the right-hand side of Eq. (16), i.e., it now is specified that

$$\frac{N_t}{N_m} = \frac{\bar{E}_t}{A_{11}}\left[\frac{\nu_{AB} + \tan^2\alpha}{\tan^2\alpha(\bar{\nu}_{tm} - \nu_{AB}) + \bar{\nu}_{tm}\,\nu_{AB} - 1}\right] + \bar{\nu}_{tm} + 2 - Z \quad (18)$$

where $Z \leqq 2$.

The quantity Z may be thought of as a "form factor" which can be varied from point to point along the dome contour. Then, for a particular value of Z_0 (the value of Z at the tangent point), the free edge deflection of the dome will match that of the cylinder. Since the deflection at the tangent point is essentially a function of the properties only at the point, Z may be increased to a maximum of 2.0 in a short distance from the tangent point. Since a balanced stress condition is obtained when $Z = 2.0$, the dome will be balanced at every point except in the immediate region of the tangent point. The problem of slope (bending rotation) discontinuity at the tangent point and the effect of a skirt attachment is discussed in the next section.

Juncture Analysis

The discontinuity stresses at the juncture of a cylinder, dome, and skirt may be evaluated by considering the section as three free bodies as indicated in Fig. 4. The edge coefficients of each component can be obtained from the integration of the equations of motion presented in the Appendix. Then, by equating the corresponding loads and displacements, the discontinuity loads may be evaluated.

To minimize the discontinuity stresses in the dome, a suitable value of Z_0 must be found. This may be accomplished by first considering the juncture of only the cylinder and the skirt. The radial deflection that would exist at the juncture of these two components may be evaluated from the edge coefficients. Letting this deflection be designated $\bar{w}_0$, Eqs. (17) and (18) may be combined to give

$$Z_0 = \frac{2\bar{E}_t\,h\,\bar{w}_0}{p\,a^2} + \frac{\bar{E}_t}{A_{11}}\left[\frac{\nu_{AB} + \tan^2\alpha_0}{\tan^2\alpha_0(\bar{\nu}_{tm} - \nu_{AB}) + \bar{\nu}_{tm}\,\nu_{AB} - 1}\right] + 2 \quad (19)$$

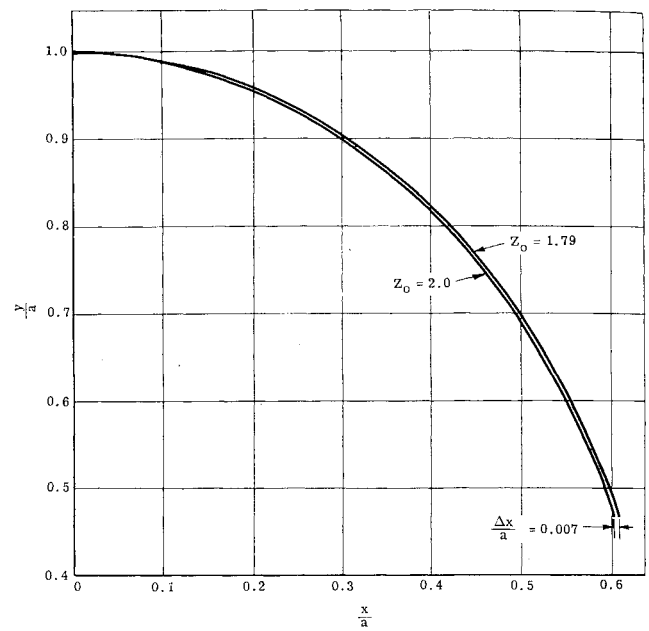

Fig. 5 Effect of Z_0 on dome contour.

This value of Z_0, then, establishes the contour of a dome such that its free edge deflection is the same as that of the cylinder-skirt combination. Although this does not ensure that the slope (bending rotation) of the dome will match that of the cylinder and skirt, the stresses resulting from a discontinuity in slope generally will be less than those caused by a deflection discontinuity. By letting the value of Z_0 vary slightly from that given by Eq. (19), a process of iteration may be used to find the value of Z_0 at which the discontinuity stresses in the dome are a minimum.

The effect of Z_0 on the dome contour is illustrated in Fig. 5, where the contours are shown terminating approximately at their inflection points. The principal difference in the contours is in the meridional radius of curvature in the region of the tangent point. The larger radius of curvature for Z_0 of 1.79 results in an increased dome height of approximately 1%.

Typical discontinuity stresses at a cylinder-skirt-dome juncture are shown in Fig. 6 for both the modified and unmodified dome contours. The nondimensional stress term is obtained by dividing the composite stress in the direction of the filament, σ_A, by the netting analysis stress, σ^*, where

$$\sigma^* = 1/h \sin\alpha\,(N_m^2 \tan^2\alpha + N_t^2)^{1/2} \quad (20)$$

For each contour, the extreme fiber stresses on both the inside and outside surfaces are shown to indicate the amount of bending stress involved.

Results

Under a program initiated by Aeronautical Systems Division and Thiokol Chemical Corporation, several 44-in.-diam filament-wound pressure vessels have been fabricated and hydrotested. Some of the instrumentation used is shown in Fig. 7, the strain gages being oriented parallel to the filaments in the outermost layers. Thus, in the cylindrical portion of the vessel, the gages measured strain in the hoop direction.

Figures 8 and 9 show a comparison of calculated and measured strains as functions of internal pressure. In general, the agreement is good, particularly in the lower stress range. At higher stresses, the material exhibits a "knee" in the stress-strain curve due to an unidirectional failure of the resin. Most of the discrepancies shown in Figs. 8 and 9 may be attributed to the neglecting of shear strains in the resin and to the assumption that the linear elastic relationships remain

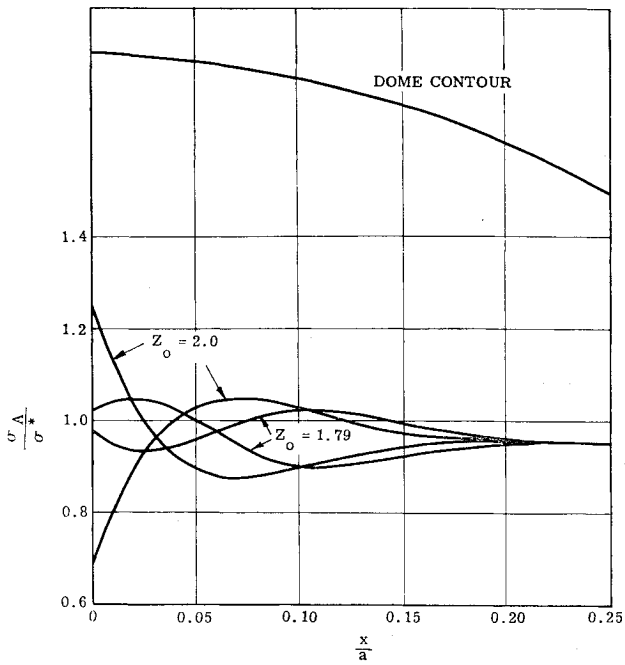

Fig. 6 Effect of Z_0 on dome stress.

valid throughout the entire stress range. Thus, the accuracy of the theoretical approach could be improved by a more rigorous formulation of the equations which would include the effects of interlaminar shear and of stress-dependent material properties.

Appendix: Derivation of Equations

A differential element of a surface of revolution is shown in Fig. 10. The displacement w and v are measured normal to the surface and along the meridian, respectively. The

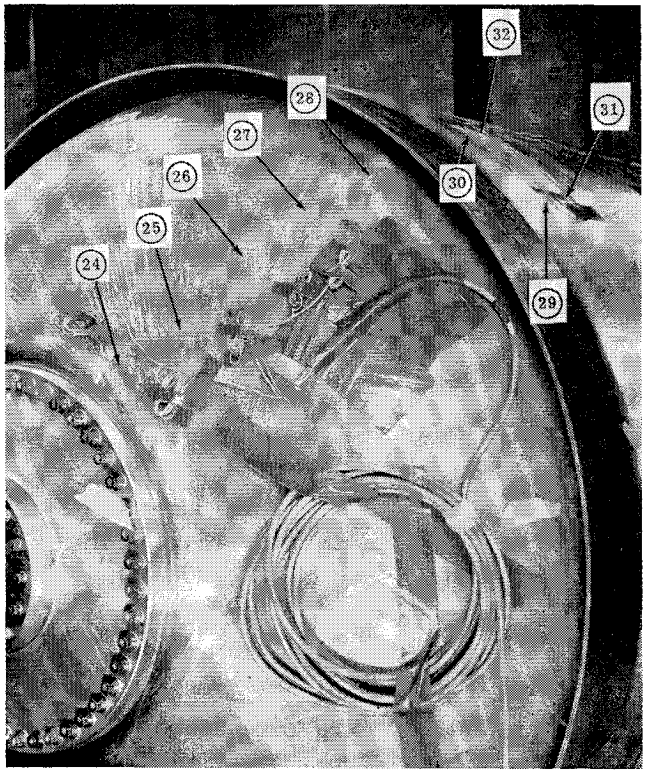

Fig. 7 Strain gage locations.

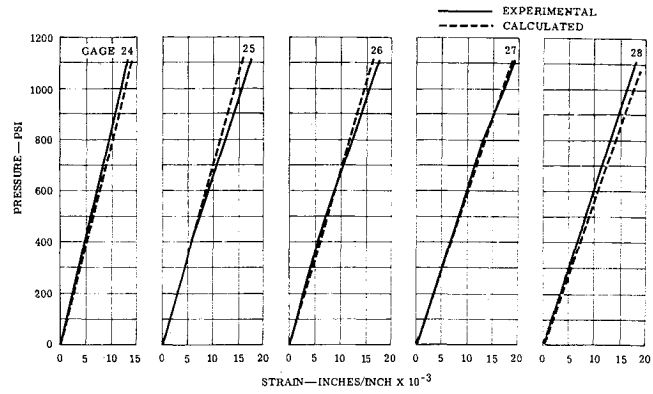

Fig. 8 Experimental and calculated strains in dome section.

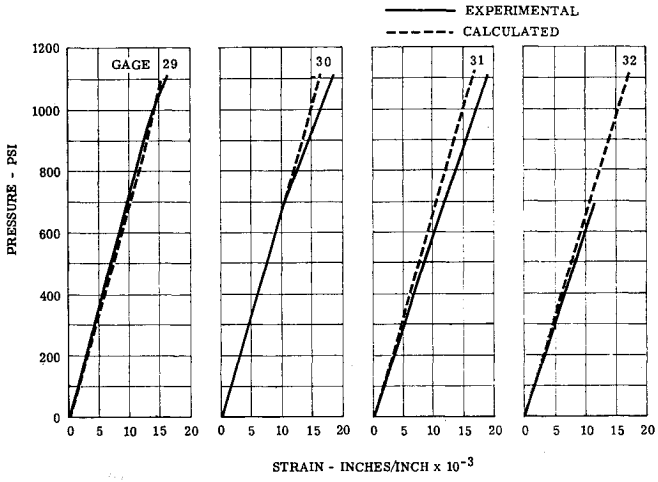

Fig. 9 Experimental and calculated strains in cylindrical section.

equations of equilibrium of an element are[4]

$$\begin{aligned} [d(y\,N_m)/d\phi] - r_m\,N_t\cos\phi - (yQ) &= 0 \\ (y\,N_m) + r_m\,N_t\sin\phi + [d(yQ)/d\phi] - y\,r_m p &= 0 \\ [d(y\,M_m)/d\phi] - r_m\,M_t\cos\phi - r_m(yQ) &= 0 \end{aligned} \qquad \text{(A1)}$$

It is assumed that at any point on the dome, the number of layers oriented at an angle α with respect to the meridian is equal to the number of layers oriented at an angle $-\alpha$ and that the absolute value of α does not vary through the thickness. It is further assumed that the layers are connected by a material which has an infinite shear rigidity.

Then, for a symmetrically loaded surface of revolution,

$$\gamma_{mt} = 0 \qquad \text{(A2)}$$

The strains due to the membrane stresses are given by

$$\begin{aligned} \epsilon_m &= (1/r_m)[(dv/d\phi) - w] \\ \epsilon_t &= (1/r_t)(v\cot\phi - w) \end{aligned} \qquad \text{(A3)}$$

Using the notation of Eq. (9),

$$\bar{E}_t = A_{22} - (1/A_{11})(A_{12})^2 \qquad \bar{\nu}_{tm} = A_{12}/A_{11}$$

and the definition that $\sigma_m = N_m/h$, Eqs. (A2) and (A3) may be substituted into the first of Eq. (4) to give

$$\frac{dv}{d\phi} = -\frac{r_m}{r_t}\bar{\nu}_{tm}\cot\phi\,v + \left(1 + \frac{r_m}{r_t}\bar{\nu}_{tm}\right)w + \frac{r_m}{yA_{11}h}(y\,N_m) \qquad \text{(A4)}$$

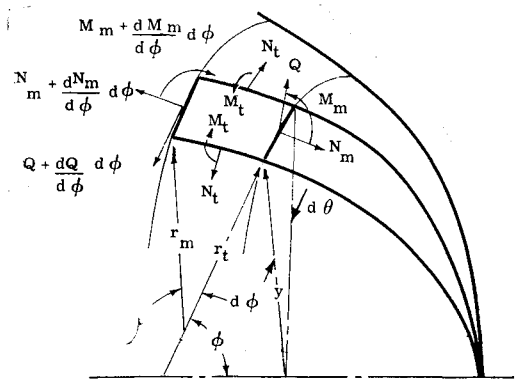

Fig. 10 Element of surface of revolution.

The rotation of a tangent to a meridian may be expressed as

$$S = (1/r_m)[v + (dw/d\phi)]$$

Then

$$dw/d\phi = r_m S - v \tag{A5}$$

The curvatures due to bending are given by

$$K_m = (1/r_m)(dS/d\phi)$$
$$K_t = (1/r_t)S \cot\phi \tag{A6}$$

The strains due to bending are

$$\epsilon_m = -K_m z \qquad \epsilon_t = -K_t z \tag{A7}$$

The bending moments are defined by

$$M_m = \int_{-h/2}^{h/2} \sigma_m z\, dz \qquad M_t = \int_{-h/2}^{h/2} \sigma_t z\, dz \tag{A8}$$

but

$$\sigma_m = A_{11}\epsilon_m + A_{12}\epsilon_t = -A_{11}K_m z - A_{12}K_t z \tag{A9}$$

Then

$$M_m = -\int_{-h/2}^{h/2} (A_{11}K_m + A_{12}K_t)\, z^2\, dz =$$
$$-\frac{h^3}{12}[A_{11}K_m + A_{12}K_t] \tag{A10}$$

$$M_m = \frac{-h^3}{12}\left[A_{11}\left(\frac{1}{r_m}\frac{dS}{d\phi}\right) + A_{12}\left(\frac{1}{r_t}S\cot\phi\right)\right]$$

In a similar manner,

$$M_t = -\frac{h^3}{12}\left[A_{12}\frac{1}{r_m}\frac{dS}{d\phi}\right) + A_{22}\left(\frac{1}{r_t}S\cot\phi\right)\Big] \tag{A11}$$

Note that it is assumed that the material properties do not vary through the thickness of the shell. From Eq. (A10), using Eq. (9),

$$\frac{dS}{d\phi} = -\frac{r_m}{r_t}\bar{\nu}_{tm}\cot\phi S - \frac{12r_m}{yh^3A_{11}}(y\,M_m) \tag{A12}$$

Substituting Eq. (A12) into Eq. (A11) gives

$$M_t = (\bar{E}_t h^3/12r_t)S\cot\phi + \bar{\nu}_{tm}M_m \tag{A13}$$

Substituting Eq. (A13) into the third of Eq. (A1) and using the relationship $y = r_t \sin\phi$,

$$\frac{d(y\,M_m)}{d\phi} = -\frac{r_m h^3 \cos^2\phi \bar{E}_t}{12y}S +$$
$$\frac{r_m}{r_t}\bar{\nu}_{tm}\cot\phi(y\,M_m) + r_m(yQ) \tag{A14}$$

Combining Eqs. (4) and (A3) and using $\sigma_t = N_t/h$

$$N_t = \bar{\nu}_{tm}N_m + \bar{E}_t h[(1/r_t)(v\cot\phi - w)] \tag{A15}$$

Substitution of Eq. (A15) into the second of Eq. (A1) gives

$$\frac{d(yQ)}{d\phi} = -\frac{r_m}{r_t}\bar{E}_t h\cos\phi v + \frac{r_m}{r_t}\bar{E}_t h\sin\phi w -$$
$$\left(1 + \frac{r_m}{r_t}\bar{\nu}_{tm}\right)(yN_m) + p\,r_m r_t \sin\phi \tag{A16}$$

Substitution of Eq. (A15) into the first of Eq. (A1) gives

$$\frac{d(y\,N_m)}{d\phi} = \frac{r_m}{y}\bar{E}_t h\cos^2\phi v - \frac{r_m}{r_t}\bar{E}_t h\cos\phi\, w +$$
$$(yQ) + \frac{r_m}{r_t}\bar{\nu}_{tm}\cot\phi(yN_m) \tag{A17}$$

Thus, the equations of motion of an orthotropic axisymmetric surface of revolution under axisymmetric loading may be expressed in the form of six linear first-order differential equations. These are summarized as follows:

$$\frac{dv}{d\phi} = -\frac{r_m}{r_t}\bar{\nu}_{tm}\cot\phi\, v + \left(1 + \frac{r_m}{r_t}\bar{\nu}_{tm}\right)w + \frac{r_m}{y\,A_{11}h}(y\,N_m)$$

$$\frac{dw}{d\phi} = r_m S - v$$

$$\frac{dS}{d\phi} = -\frac{r_m}{r_t}\bar{\nu}_{tm}\cot\phi S - \frac{12r_m}{y\,h^3A_{11}}(y\,M_m)$$

$$\frac{d\,(yM_m)}{d\phi} = -\frac{r_m h^3\cos^2\phi\bar{E}_t}{12\,y}S + \frac{r_m}{r_t}\bar{\nu}_{tm}\cot\phi(yM_m) + r_m\,(yQ)$$

$$\frac{d(yQ)}{d\phi} = \frac{-r_m}{r_t}\bar{E}_t h\cos\phi v + \frac{r_m}{r_t}\bar{E}_t h\sin\phi w -$$
$$\left(1 + \frac{r_m}{r_t}\bar{\nu}_{tm}\right)(y\,N_m) + p\,r_m r_t\sin\phi$$

$$\frac{d(y\,N_m)}{d\phi} = \frac{r_m}{y}\bar{E}_t h\cos^2\phi v - \frac{r_m}{r_t}\bar{E}_t h\cos\phi\, w +$$
$$(yQ) + \frac{r_m}{r_t}\bar{\nu}_{tm}\cot\phi(y\,N_m)$$

These equations may be solved by numerical integration using a digital computer.

References

[1] Dietz, A. G. H., *Engineering Laminates* (John Wiley and Sons, New York, 1949), Chap. 1.

[2] DeHaven, C. C., "Development of a generatrix for pressure vessel dome closures with minimum hoop stresses in the surfaces," Allegany Ballistics Lab. Rept. X-39 (1959).

[3] Kitzmiller, A. H., DeHaven, C. C., and Young, R. E., "Design considerations for spiralloy glass-reinforced filament-wound structures as rocket inert parts," ARS Preprint 983-59 (November 1959).

[4] Timoshenko, S., *Theory of Plates and Shells* (McGraw-Hill Book Co., Inc., New York, 1940). 1st ed., p. 450.